SENSITIVITY ANALYSIS OF A COUPLED HYDRO-MECHANICAL PALEO-CLIMATE MODEL OF DENSITY-DEPENDENT GROUNDWATER FLOW IN DISCRETELY FRACTURED CRYSTALLINE ROCK

Stefano D. Normani and Jonathan F. Sykes
Department of Civil and Environmental Engineering, University of Waterloo
Waterloo, Ontario, Canada

ABSTRACT

A high resolution three-dimensional sub-regional scale (104 km^2) density-dependent, discretely fractured groundwater flow model with hydro-mechanical coupling and pseudo-permafrost was developed from a larger 5734 km^2 regional-scale groundwater flow model of a Canadian Shield setting. The objective of the work is to determine the sensitivity of modelled groundwater system evolution to the hydro-mechanical parameters.

The discrete fracture dual continuum numerical model FRAC3DVS-OPG was used for all simulations. A discrete fracture network model delineated from surface features was superimposed onto an approximate 790 000 element domain mesh with approximately 850 000 nodes. Orthogonal fracture faces (between adjacent finite element grid blocks) were used to best represent the irregular discrete fracture zone network. Interconnectivity of the permeable fracture zones is an important pathway for the possible migration and subsequent reduction in groundwater and contaminant residence times. The crystalline rock matrix between these structural discontinuities was assigned mechanical and flow properties characteristic of those reported for the Canadian Shield. The variation of total dissolved solids with depth was assigned using literature data for the Canadian Shield. Performance measures for the sensitivity analysis include equivalent freshwater heads, environmental heads, linear velocities, and depth of penetration by conservative non-decaying tracers released at the surface.

A 121 000 year North American continental scale paleo-climate simulation was applied to the domain with ice-sheet histories estimated by the University of Toronto Glacial Systems Model (UofT GSM). Hydro-mechanical coupling between the rock matrix and the pore fluid, due to the ice sheet normal stress, was included in the simulations. The flow model included the influence of vertical strain and assumed that areal loads were homogeneous. Permafrost depth was applied as a permeability reduction to both three-dimensional grid blocks and fractures that lie within the time varying permafrost zone. Values of ice sheet normal stress and proglacial lake depth from the UofT GSM were applied to the sub-regional model as surface boundary conditions using a freshwater head equivalent to the normal stress imposed by the ice sheet at its base. The sensitivity of glacial meltwater penetration to different conceptualizations of hydro-mechanical properties were investigated.

1. INTRODUCTION

Potential host rock for a deep geologic repository (DGR) for used nuclear fuel includes the crystalline rock of the Canadian Shield. Both the safety case and safety assessment of a DGR must consider the impact on the repository of glaciation. Over the past 900 000 years, the Canadian Shield has experienced approximately 9 episodes of complete glaciation. During the glaciation cycles, the entire Canadian land mass has been covered by a series of continental ice-sheets whose maximum thickness reached 4 km [1]. This paper undertakes a sensitivity analysis of a coupled hydromechanical model that is used to assess the impact of mechanical loading due to glaciation on a granitic rock at a hypothetical site in the Canadian Shield.

Climate change and glaciation are not only a concern for the Canadian nuclear fuel waste disposal concept, but also for the Swedish [2, 3] and Finnish concepts [4]. Peltier [1] and Marshall et al. [5] have developed glaciological reconstructions of the Laurentide Ice-Sheet using numerical models. During ice-sheet advance, a repository site would evolve from periglacial to subglacial conditions. Permafrost several hundred metres thick develops in advance of the ice-sheet [1].

2. HYDROMECHANICAL COUPLING

One-dimensional vertical loading and unloading due to glaciation, erosion, or deposition, is a common simplification that can be applied in hydromechanical coupling; this coupling is applied to porous media, ignoring mechanical effects on fractures [6, 7, 8]. Assuming that the porous media, solid grains, and pore fluid are all compressible, the specific storage S_s is defined as:

$$S_s = \rho\, g \left[\left(\frac{1}{K} - \frac{1}{K_s} \right) (1-\lambda) + n \left(\frac{1}{K_f} - \frac{1}{K_s} \right) \right], \quad \lambda = \frac{2\alpha(1-2\nu)}{3(1-\nu)}, \quad \alpha = 1 - \frac{K}{K_s} \qquad (1)$$

where ρ is the fluid density [M/L^3]; g is the gravitational constant [L/T^2]; K is the drained bulk modulus of the porous media [M/T^{2}L]; K_s is the bulk modulus of the solids in the porous media [M/T^{2}L]; K_f is the bulk modulus of the pore fluid [M/T^{2}L]; α is the Biot coefficient [/]; and ν is the Poisson's ratio [/]. The bulk modulus K is defined as the reciprocal of compressibility, therefore $K = 1/\beta$ as presented in Jaeger et al. [8]

The effect of mechanically loading the surface of a porous media is to transfer the load to both the porous media, and the pore fluid; the effects of mechanical loading and pore pressure affect each other, and are thus coupled. The groundwater flow equation can be modified to account for one-dimensional hydromechanical coupling as follows:

$$\frac{\partial}{\partial x_i} \left[K_{ij} \left(\frac{\partial h}{\partial x_j} + \rho_r \frac{\partial z}{\partial x_j} \right) \right] \pm Q = S_s \frac{\partial h}{\partial t} - \frac{S_s\, \zeta}{\rho\, g} \frac{\partial \sigma_{zz}}{\partial t} \qquad i,j = 1,2,3 \qquad (2)$$

where K_{ij} is the porous media hydraulic conductivity tensor [L/T]; h is the freshwater head [L]; ρ_r is the relative fluid density [/]; g is the gravitational constant [L/T^2]; z is the fluid elevation [L]; ζ

is the one-dimensional loading efficiency [/]; and σ_{zz} is the vertical stress [M/LT^2]. The loading efficiency is further defined as [6, 7]:

$$\zeta = \frac{B(1+\nu)}{3(1-\nu)-2\alpha B(1-2\nu)}, \quad B = \frac{\left(\frac{1}{K}-\frac{1}{K_s}\right)}{\left(\frac{1}{K}-\frac{1}{K_s}\right)+n\left(\frac{1}{K_f}-\frac{1}{K_s}\right)} \tag{3}$$

where B is the Skempton coefficient and physically represents the ratio of change in fluid pressure to a change in mean effective stress under undrained conditions [7].

3. SUB-REGIONAL MODEL

Pore water at repository horizon in granitic rock of the Canadian Shield can have high total dissolved solids concentrations and hence elevated water density. The analysis of mechanical loading due to glaciation on groundwater also thus must include the assessment of density-dependent flow. The solution methodology for the analysis of hydromechanical coupling with density-dependent flow was developed in Normani et al. [9]. Both steady-state and pseudo steady-state simulations need to be run prior to paleoclimate simulations. For a given modelling scenario, a steady-state simulation without total dissolved solids (TDS) is run using FRAC3DVS-OPG. The resulting freshwater heads from the steady-state simulation are modified to account for the presence of high TDS, where the development of the initial TDS distribution is described in Section 3.2. The adjusted freshwater heads and initial TDS distribution form the initial conditions for a 1 Ma transient simulation, whose final state at 1 Ma represents a pseudo steady-state. A 1 Ma time frame allows for the higher conducting portions of the domain, namely the near surface and fracture zones, to flush with fresh water entering the domain from the top boundary and for diffusive losses of TDS to take place from the matrix to the fracture zones. The resulting pseudo steady-state freshwater heads and TDS distribution are used as the initial conditions for the paleoclimate simulations. The modelling domain is shown in Figure 1.

3.1. Spatial Discretization

The three-dimensional sub-regional domain of a hypothetical DGR site on the Canadian Shield was discretized into 847 080 nodes, and 789 887 brick elements, covering an area of 104 km^2. The grid is orthogonal with each equivalent porous medium (EPM) block having the same planimetric dimensions of 50 m by 50 m and was vertically discretized into 19 layers. The top of model layer 19 is defined by a digital elevation model (DEM) using the linear interpolation method within the Spatial Analyst package of ArcView 3.2a. Layers 1 through 14 inclusive have a constant thickness, while Layers 15 through 19 have a variable thickness which depends on the elevation of surface topography for the hypothetical site.

3.2. Initial Conditions

The paleoclimate simulations require coupled density-dependent flow and transport due to the high TDS concentrations found deep in the Canadian Shield. An initial TDS distribution is required for the pseudo steady-state model. An equation for TDS versus depth d for groundwaters from the Canadian Shield, based on Figure 2b in Frape and Fritz [10], is presented as Equation (4) where

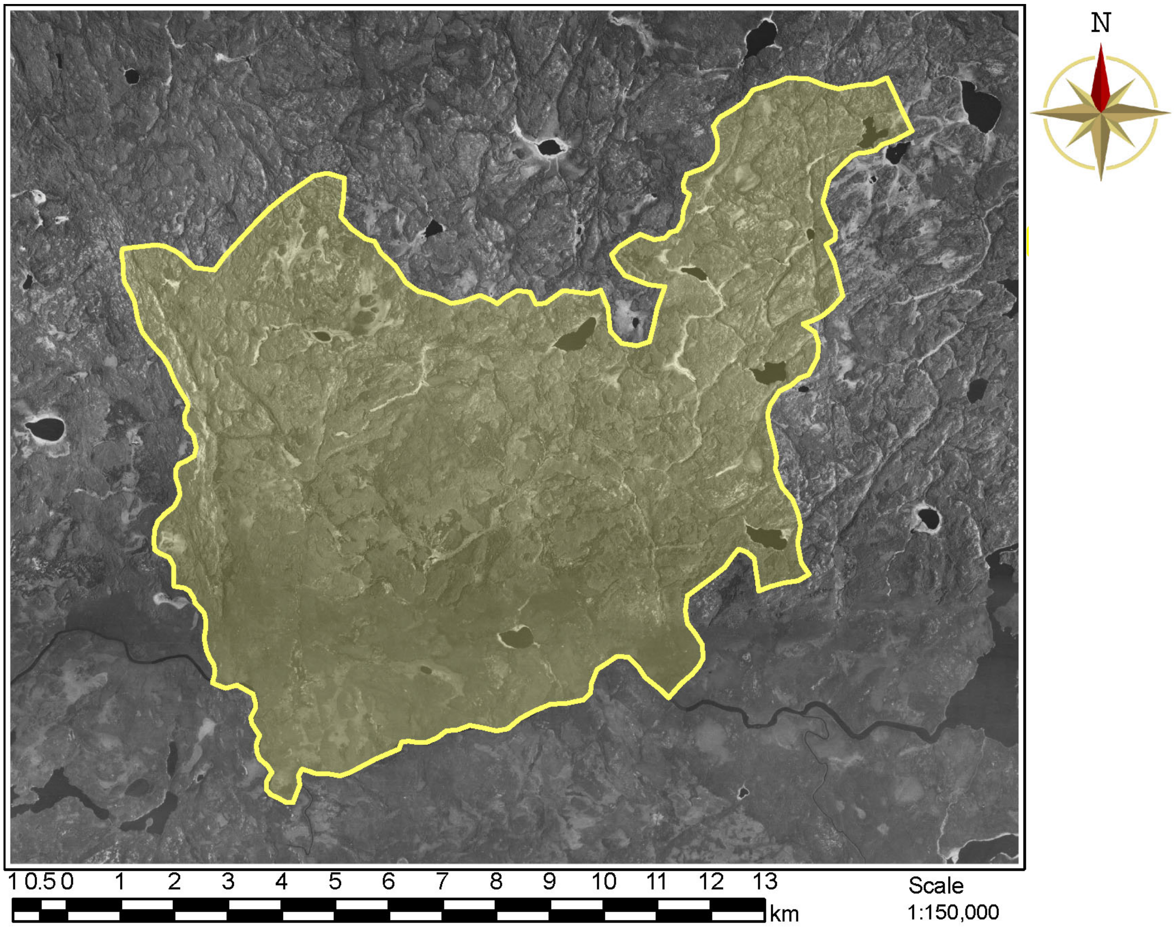

Figure 1. Sub-regional modelling domain and aerial photo.

TDS is in units of g/L. The exponent of 0.001981697 is required to ensure TDS concentrations of 1 g/L at surface, and 300 g/L at a depth of 1250 m.

$$TDS = \begin{cases} 10^{0.001981697d}, & \text{for } d \leq 1250\,\text{m}; \\ 300, & \text{for } d > 1250\,\text{m}. \end{cases} \tag{4}$$

Setting an upper bound for the TDS distribution as an initial condition allows recharge waters to reduce the TDS concentrations in fractures, and in the nearby rock matrix during the pseudo steady-state simulations, providing a constrained initial condition for the paleoclimate simulations.

3.3. Boundary Conditions

For the steady-state and pseudo steady-state models, specified head is applied to surface nodes associated with water features, while a recharge rate of 1.0 mm/a is applied elsewhere across the top of the model. A zero-flux boundary condition for flow is applied to the model's sides and bottom. Due to low permeabilities at depth and high pore water salinities, negligible vertical flow is expected at the base of the domain. Horizontal domain boundaries were chosen based on topography, and as such, may not be representative of no flow conditions during glacial advancements or retreats across the domain, however these movements across the domain within hundreds of years and are likely to only significantly affect horizontal flow in the higher permeability regions and only for a time period that is small relative to the 120 ka paleohydrogeologic simulation.

For the paleoclimate simulations, a tracer associated with water entering the groundwater model from the top surface is used to investigate glacial meltwater migration in the subsurface during and subsequent to a glaciation and deglaciation episode. A Cauchy boundary condition at the model's top surface is used with a tracer concentration of unity.

Peltier [1] and Peltier [11] developed North American continental-scale models of glaciation over the last 120 000 yrs; model NN2778 is used for the analyses of this study. A plot of nn2778 Glacial Systems Model (GSM) model outputs, including ice thickness and permafrost depth, for the grid cell containing the sub-regional modelling domain are shown in Figure 2. The ice thickness, lake depth, and permafrost depth outputs are applied explicitly to the paleoclimate groundwater flow simulations.

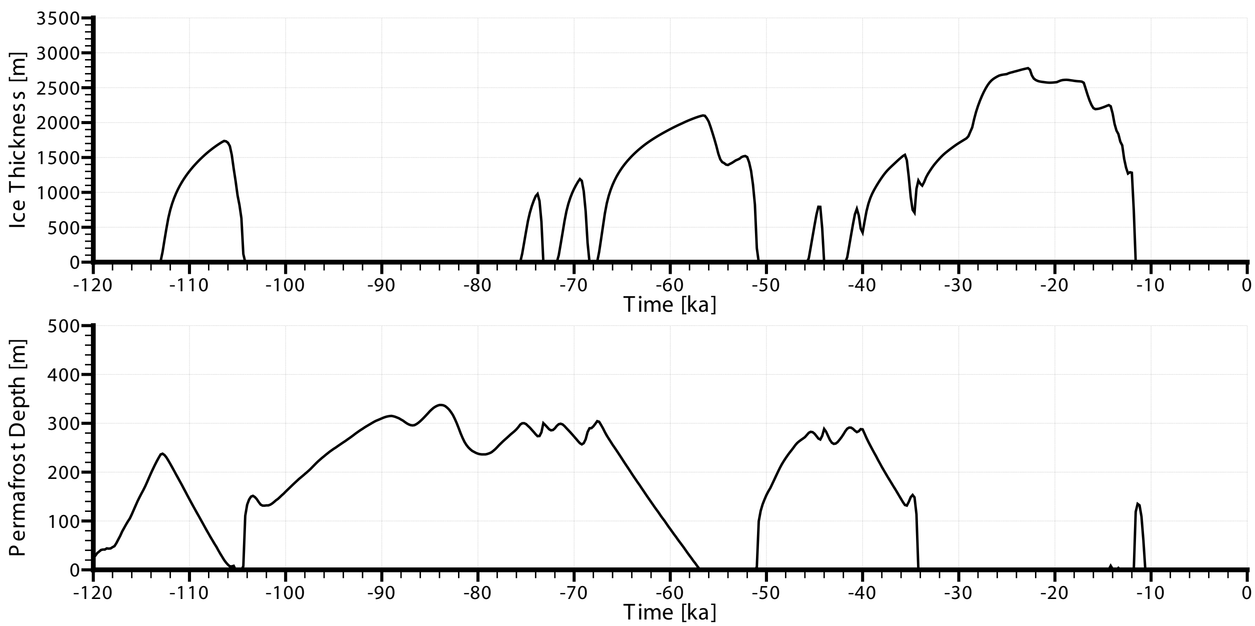

Figure 2. Plots of ice thickness and permafrost depth versus time for the nn2778 GSM grid block containing the sub-regional modelling domain, provided by Peltier [11].

3.4. Fracture Network Model

Discrete fracture zones are an important attribute that must be considered in the analysis of a DGR site in granitic rock of the Canadian Shield. Srivastava [12] developed a framework for generating equally likely discrete fracture zone models. The first unconditioned fracture network model (FNM) for the hypothetical site from Srivastava [13] was chosen for all paleoclimate simulations. The FNM was then mapped onto an orthogonal brick element mesh whereby planar quadrilateral elements are used to represent fracture zone network geometry. The resulting orthogonal FNM is shown in Figure 3.

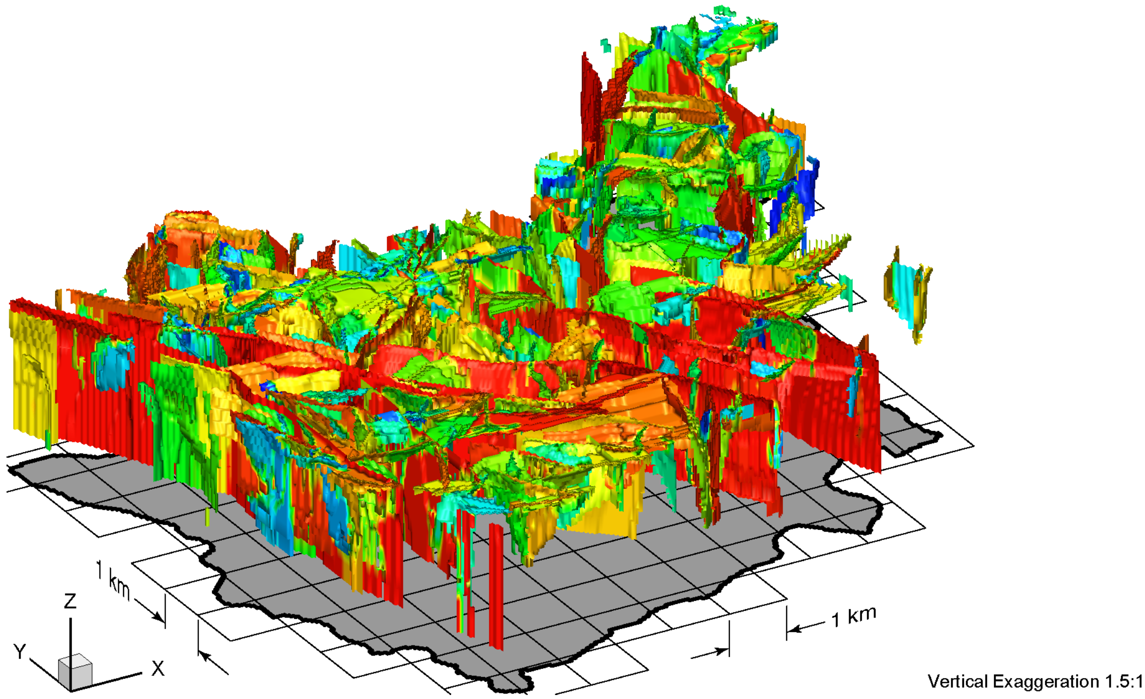

Figure 3. 3-D perspective view of discretized FNM.

3.5. Properties

Properties for the paleoclimate simulations are provided in Table 1. The values for Young's Modulus E and Poisson's ratio ν are provided in Chan and Stanchell [14]. The calculation of specific storage S_s and one-dimensional loading efficiency ζ assume the Biot coefficient $\alpha = 0.73$ [14], and a freshwater fluid compressibility of $4.4 \times 10^{-10}\,\mathrm{Pa}^{-1}$. Fracture properties for solute transport include a longitudinal dispersivity of 250 m, and a transverse dispersivity of 25 m. Dispersivities for the matrix include a longitudinal dispersivity of 50 m, a transverse horizontal dispersivity of 5 m and a transverse vertical dispersivity of 0.5 m. A free solution diffusion coefficient of $1.2 \times 10^{-9}\,\mathrm{m}^2/\mathrm{s}$ is used for both the brine and tracer.

Fracture zone permeability was assumed to decrease with depth from a value of approximately $1 \times 10^{-13}\,\mathrm{m}^2$ at surface to $1 \times 10^{-16}\,\mathrm{m}^2$ at depths of 1500 m. The permafrost depths were used to select any FRAC3DVS-OPG grid block whose top face was within the permafrost zone for each time step. A permafrost hydraulic conductivity of 5×10^{-11} m/s was applied and assumed to be valid for a fractured rock system McCauley et al. [15]. Any fracture which is adjacent to a hexahedral element whose permeability has been reduced due to the presence of permafrost is itself subject to the same permeability reduction.

4. PALEOCLIMATE SIMULATIONS

A steady-state simulation was performed, followed by a pseudo steady-state density-dependent simulation, which was used as the initial conditions for the paleoclimate simulations. The purpose of pseudo steady-state density-dependent simulations is to allow the groundwater system to equili-

Table 1. Sub-regional model properties for paleoclimate simulations with density-dependent and hydro-mechanical coupling.

Layer	Depth Range [m]	k_H [m^2]	k_V [m^2]	n [/]	TDS [g/L]	ρ [kg/m^3]	E [GPa]	ν [/]	S_s [m^{-1}]	ζ [/]
19	0–10	1.0×10^{-13}	1.0×10^{-12}	0.003	1.02	1000.7	20.0	0.25	3.76×10^{-7}	0.80
18	10–30	1.0×10^{-14}	1.0×10^{-13}	0.003	1.10	1000.7	20.0	0.25	3.76×10^{-7}	0.80
17	30–70	9.5×10^{-16}	9.5×10^{-15}	0.003	1.26	1000.8	20.0	0.25	3.76×10^{-7}	0.80
16	70–150	2.7×10^{-16}	2.7×10^{-15}	0.003	1.68	1001.1	20.0	0.25	3.76×10^{-7}	0.80
15	150–250	5.6×10^{-17}	5.6×10^{-16}	0.003	2.56	1001.7	30.0	0.25	2.55×10^{-7}	0.78
14	250–350	1.4×10^{-17}	1.4×10^{-16}	0.003	4.03	1002.7	30.0	0.25	2.56×10^{-7}	0.78
13	350–450	4.7×10^{-18}	4.7×10^{-18}	0.003	6.37	1004.2	60.0	0.25	1.34×10^{-7}	0.75
12	450–550	2.0×10^{-18}	2.0×10^{-18}	0.003	10.05	1006.7	60.0	0.25	1.35×10^{-7}	0.75
11	550–625	1.1×10^{-18}	1.1×10^{-18}	0.003	14.81	1009.9	60.0	0.25	1.35×10^{-7}	0.75
10	625–675	8.0×10^{-19}	8.0×10^{-19}	0.003	19.54	1013.0	60.0	0.25	1.36×10^{-7}	0.75
9	675–725	6.3×10^{-19}	6.3×10^{-19}	0.003	24.55	1016.4	60.0	0.25	1.36×10^{-7}	0.75
8	725–775	5.1×10^{-19}	5.1×10^{-19}	0.003	30.84	1020.6	60.0	0.25	1.37×10^{-7}	0.75
7	775–825	4.2×10^{-19}	4.2×10^{-19}	0.003	38.74	1025.8	60.0	0.25	1.37×10^{-7}	0.75
6	825–875	3.6×10^{-19}	3.6×10^{-19}	0.003	48.67	1032.4	60.0	0.25	1.38×10^{-7}	0.75
5	875–950	3.0×10^{-19}	3.0×10^{-19}	0.003	65.26	1043.5	60.0	0.25	1.40×10^{-7}	0.75
4	950–1050	2.4×10^{-19}	2.4×10^{-19}	0.003	98.38	1065.6	60.0	0.25	1.43×10^{-7}	0.75
3	1050–1200	1.9×10^{-19}	1.9×10^{-19}	0.003	179.62	1119.7	60.0	0.25	1.50×10^{-7}	0.75
2	1200–1400	1.5×10^{-19}	1.5×10^{-19}	0.003	269.40	1179.6	60.0	0.25	1.58×10^{-7}	0.75
1	1400–1600	1.3×10^{-19}	1.3×10^{-19}	0.003	300.00	1200.0	60.0	0.25	1.61×10^{-7}	0.75

brate from the initial assumed TDS distribution. Solute free recharge water tends to mix and dilute the interconnected fracture zones and reduce TDS in adjacent matrix blocks.

The first paleoclimate simulation uses the parameters listed in Table 1, and represents the base-case analysis. Scenario 1 uses the nn2778 glaciation scenario, with decreasing fracture zone permeability with depth, a computed one-dimensional loading efficiency, and coupled density-dependent flow and transport. Scenario 2 is identical to Scenario 1, but applies a one-dimensional loading efficiency $\zeta = 0$ to determine the sensitivity of glacial water infiltration to the loading efficiency term in the groundwater flow equation. Similarly, Scenario 3 applies a one-dimensional loading efficiency $\zeta = 1$.

4.1. Simulation Results

A tracer of unit concentration is applied as a Cauchy boundary condition to all inflow surface nodes at the beginning of the paleoclimate simulation. This tracer is used to characterize the migration, from the surface by recharge water that occurs during the paleoclimate simulation; the recharge water includes glacial meltwater. A cumulative density function of tracer depth for the 5% isochlor throughout the domain for all scenarios is provided in Figure 4.

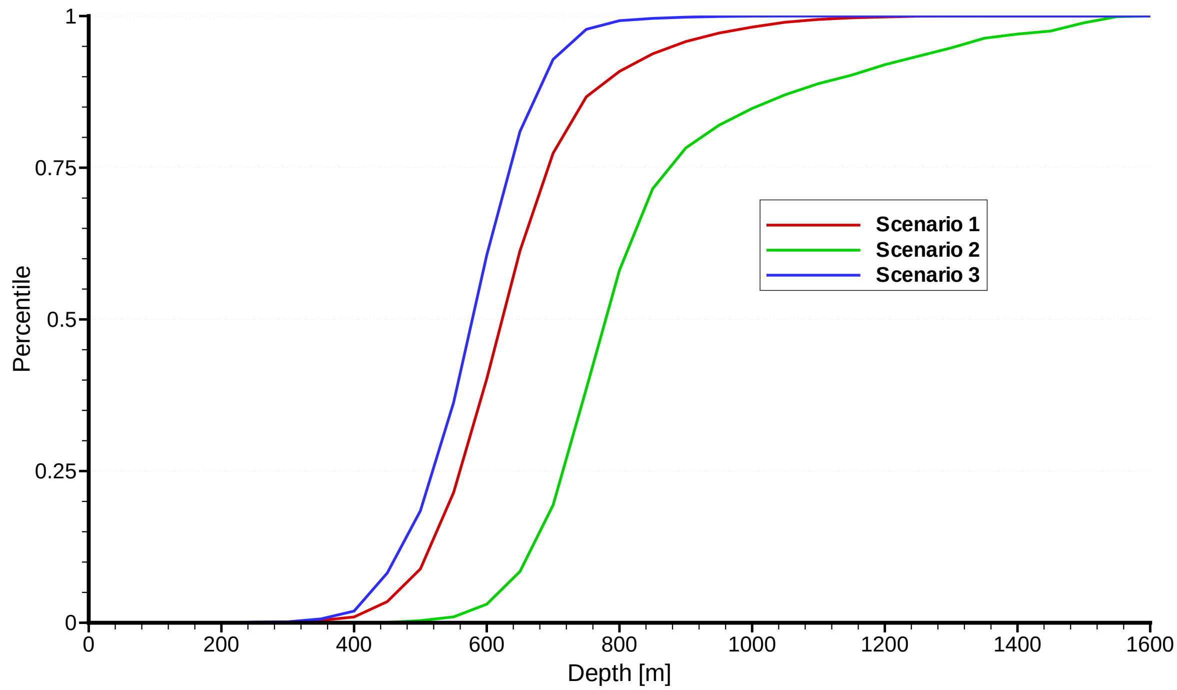

Figure 4. Depth of 5 % tracer isochlor during 120 ka paleoclimate simulation for scenarios.

Density corrected environmental heads for the domain at the end of the paleoclimate simulation are shown in Figure 5. Tracer concentrations for the modelling domain are presented in Figure 6 at the end of the 120 ka simulation; the tracer is predominantly in the matrix with some tracer appearing in fractures.

Scenario 2 investigates the role of hydromechanical coupling, by setting the one-dimensional loading efficiency, $\zeta = 0$. The environmental heads are shown in Figure 7. Significant differences in heads occur during the advance and retreat phase of the ice-sheet between Scenario 2 and Scenario 1, however, by the end of the simulation, the differences are lessened with the heads of Scenario 2 slightly greater at depth than for Scenario 1. The tracer, as shown in Figure 8 and Figure 4, has migrated deeper into the subsurface as compared to Scenario 1, due to the increased downward vertical gradients during the paleoclimate simulation resulting from ignoring hydromechanical coupling.

Scenario 3 investigates the role of hydromechanical coupling, by setting the one-dimensional loading efficiency, $\zeta = 1$; this will not permit large vertical gradients to develop because the heads in the model are either nearly uniformly increased or decreased throughout a water column by mechanical loading and unloading, depending on the surface loading condition. The environmental heads are shown in Figure 9. Significant differences in heads occur during the advance and retreat phase of the ice-sheet between Scenario 3 and Scenario 1. Vertical gradients are lesser in Scenario 3 as compared to Scenario 1. By the end of the simulation, the differences are lessened with the heads of Scenario 3 slightly less at depth than for Scenario 1. The tracer, as shown in Figure 10

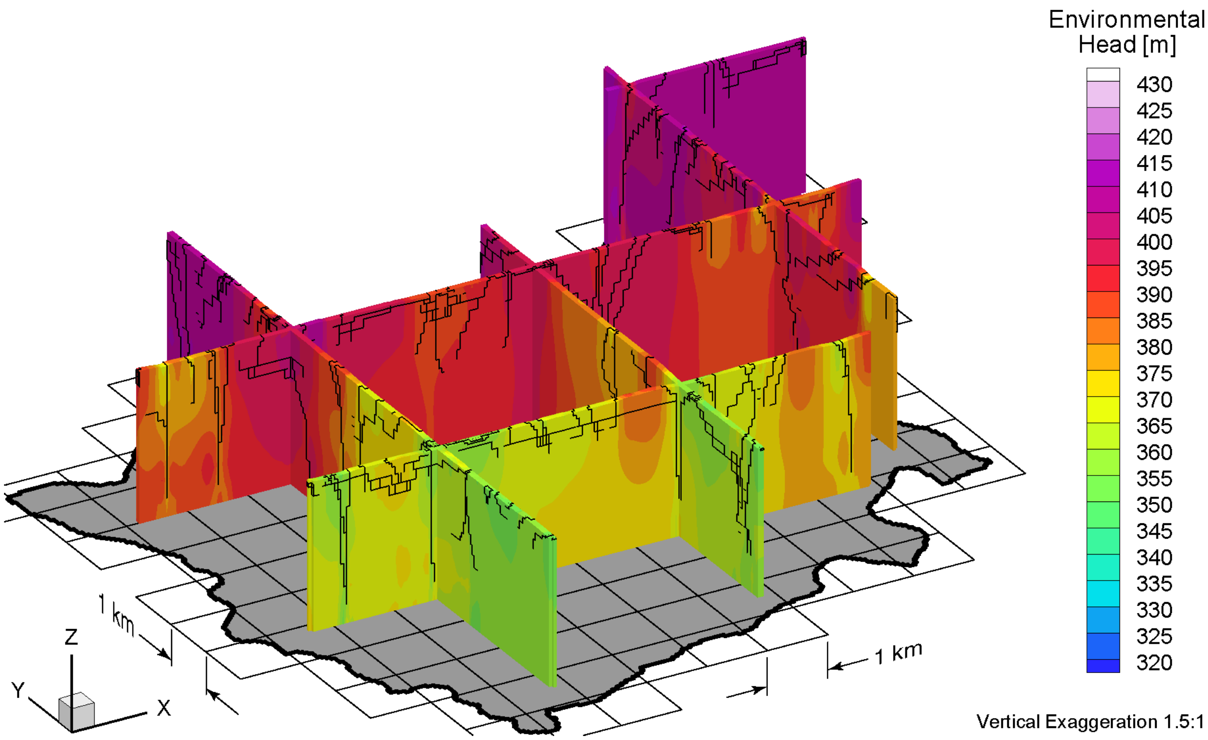

Figure 5. Environmental heads at end of 120 ka paleoclimate simulation for computed one-dimensional loading efficiency.

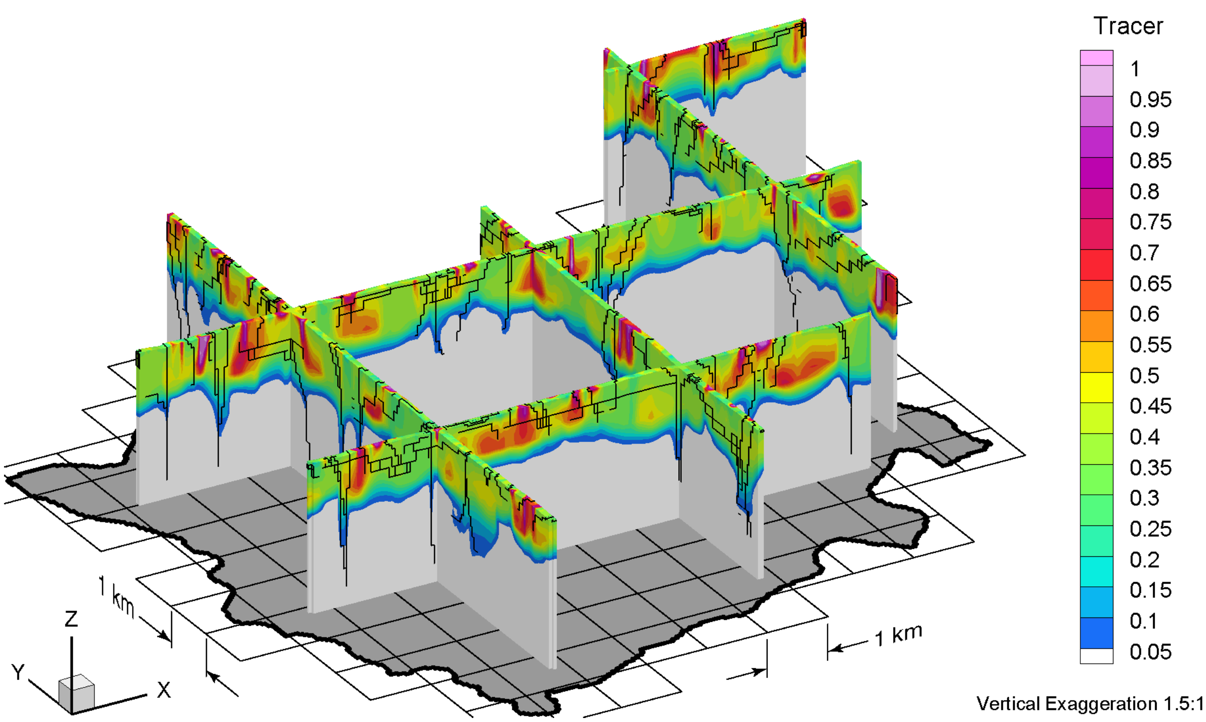

Figure 6. Migration of unit tracer during 120 ka paleoclimate simulation for computed one-dimensional loading efficiency.

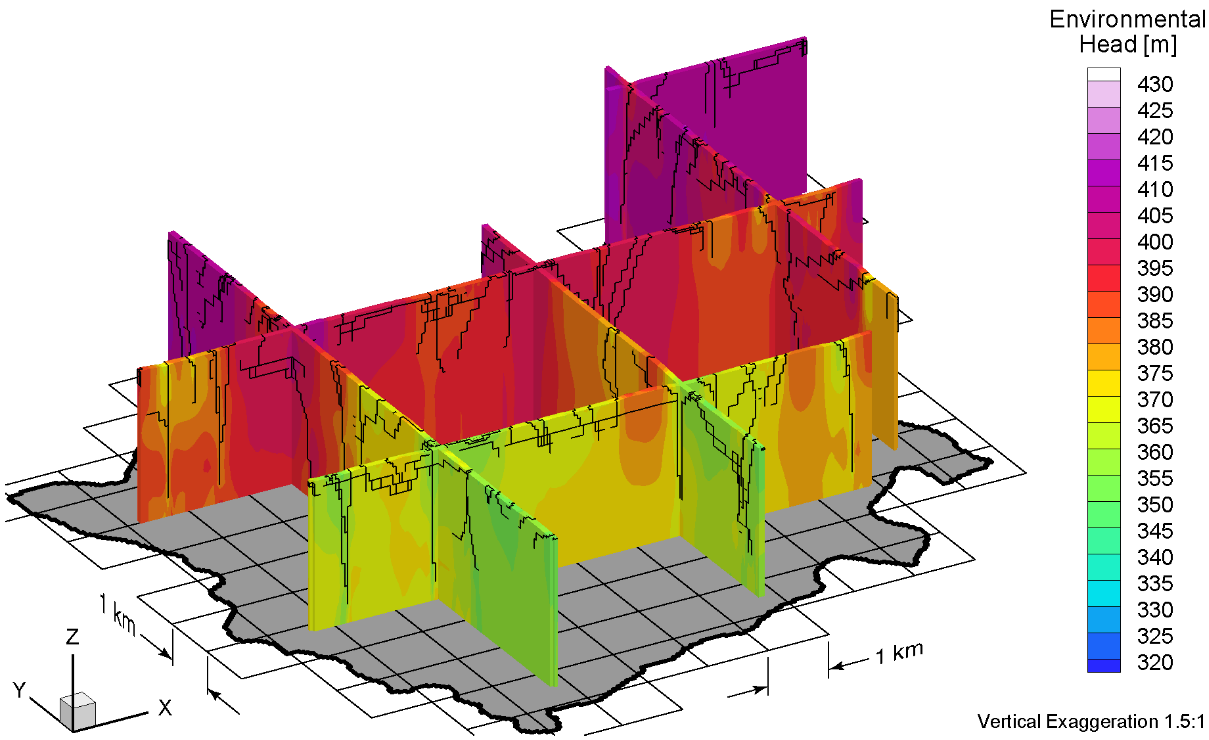

Figure 7. Environmental heads at end of 120 ka paleoclimate simulation for one-dimensional loading efficiency $\zeta = 0$.

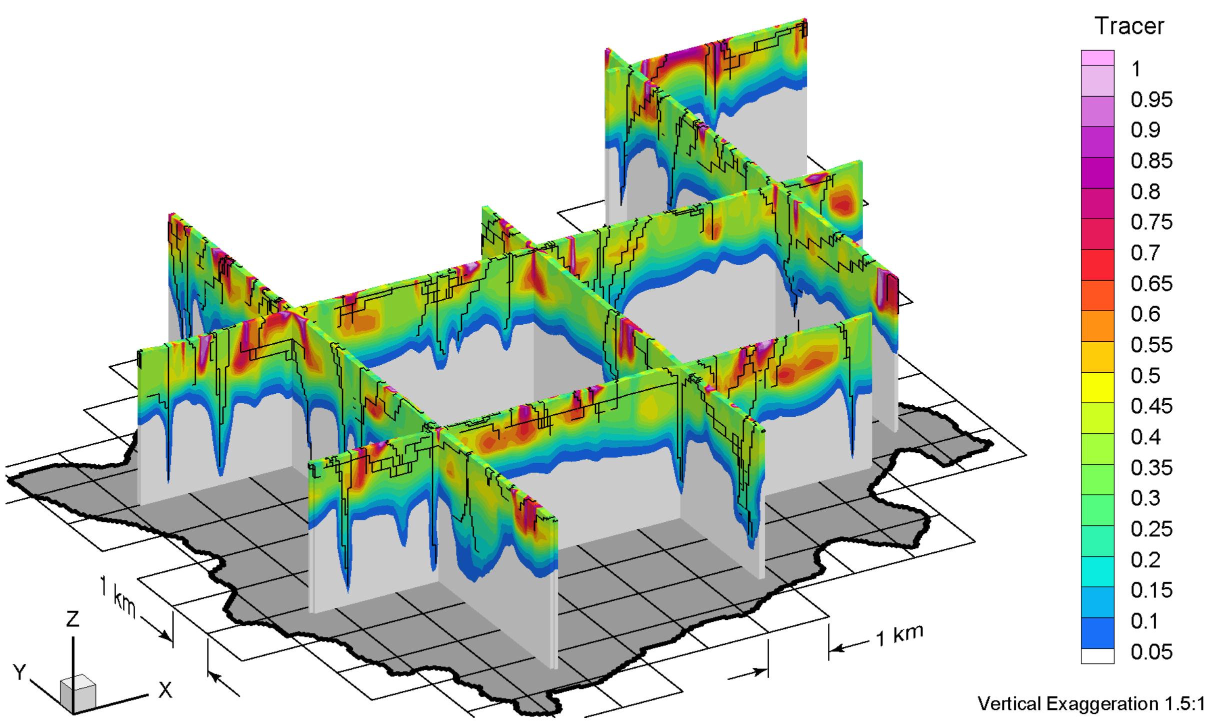

Figure 8. Migration of unit tracer during 120 ka paleoclimate simulation for one-dimensional loading efficiency $\zeta = 0$.

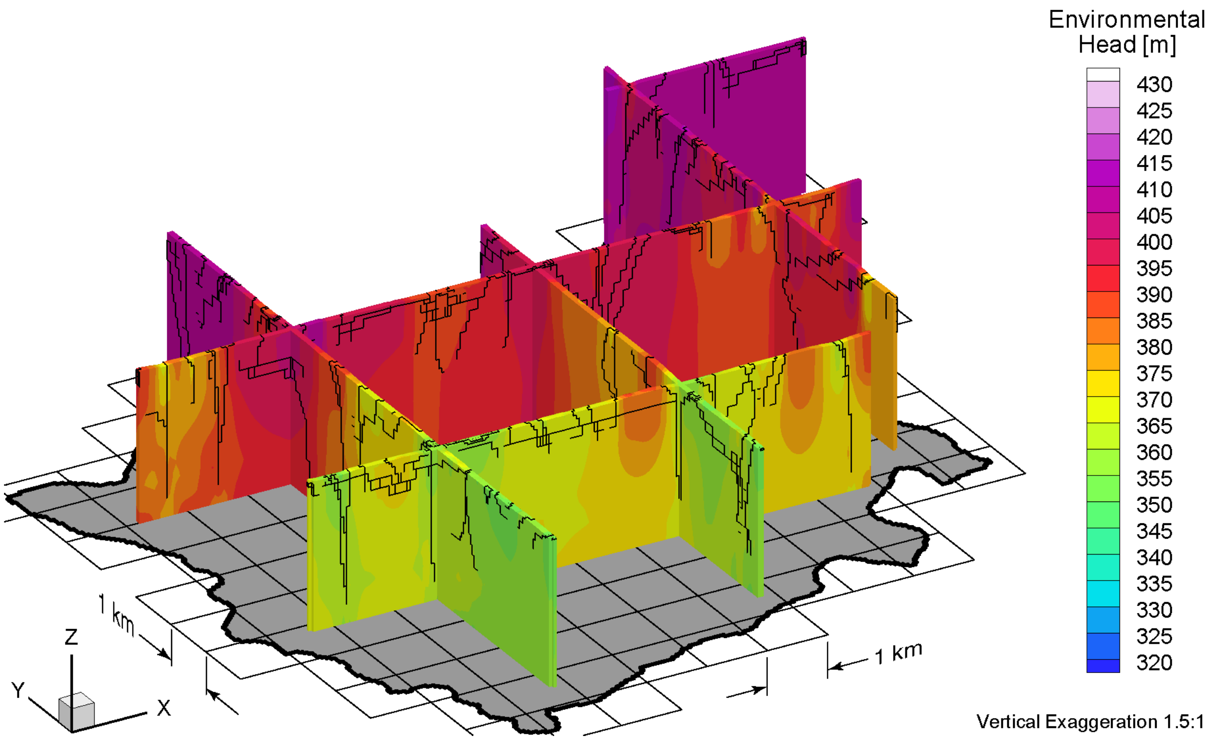

Figure 9. Environmental heads at end of 120 ka paleoclimate simulation for one-dimensional loading efficiency $\zeta = 1$.

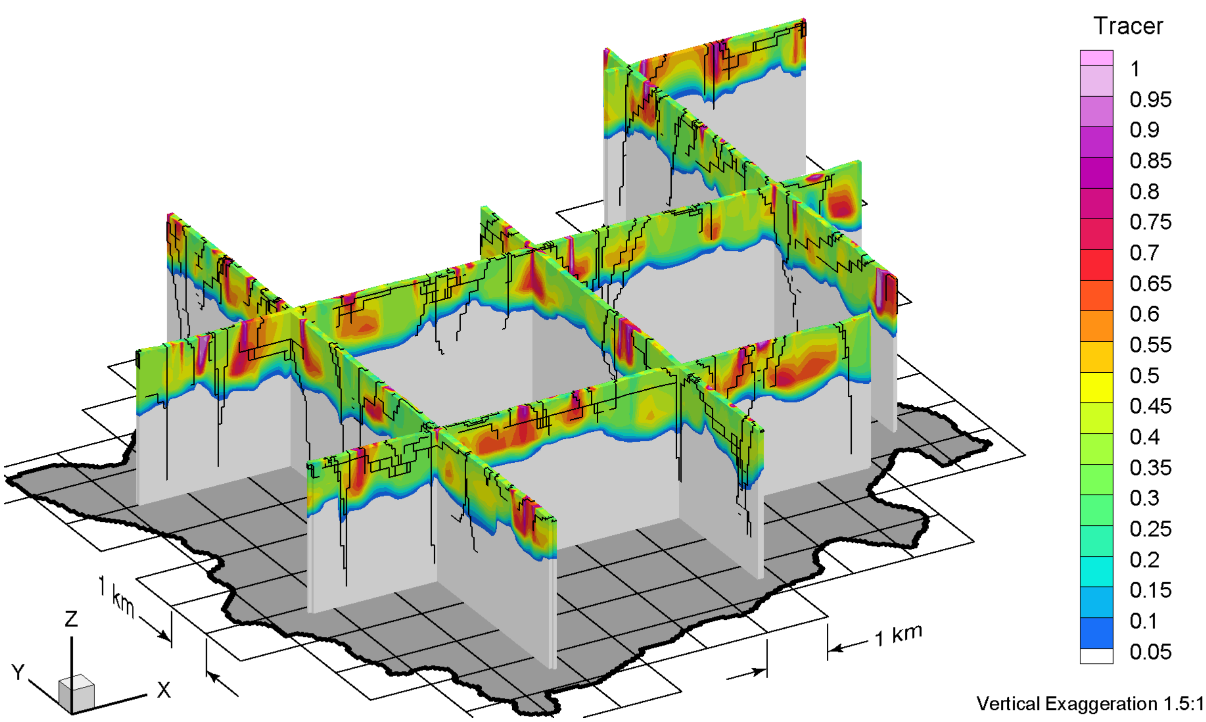

Figure 10. Migration of unit tracer during 120 ka paleoclimate simulation for one-dimensional loading efficiency $\zeta = 1$.

and Figure 4, has migrated shallower into the subsurface as compared to Scenario 1, most notably in the fractures due to the decreased vertical gradients during the paleoclimate simulation.

Figure 4 shows that the median range in tracer depth for the 5% isochlor is approximately 200 m between Scenario 2 and Scenario 3, representing a one-dimensional loading efficiency of $\zeta = 0$ and $\zeta = 1$ respectively. The shape of the CDF, in addition to Figure 6, Figure 8, and Figure 10 illustrate that the deepest tracer penetration is associated with fracture zones which represent singular, highly conductive and interconnected features. In addition, the upper portion of the CDF in Figure 4 representing the 75^{th} to 100^{th} percentile, is strongly weighed towards tracer depths associated with fracture zones, especially for Scenario 1 and Scenario 3; this is also visible in Figure 6 and Figure 10 respectively. The differences between Figure 6, Figure 8, and Figure 10 demonstrate that hydromechanical coupling is an important process that should be considered during long-term groundwater simulations for groundwater domains influenced by paleoclimate conditions. The depth of tracer migration within fracture zones is influenced by hydromechanical coupling.

5. SUMMARY AND CONCLUSIONS

Transient hydraulic head distributions during glaciation influence the evolution of the groundwater system; a key process is hydromechanical coupling. Hydromechanical coupling is an important mechanism, which affects hydraulic gradients during a glaciation event. The choice of hydromechanical coupling has significant influences on unit tracer migration and the depth of penetration by recharging meltwater. The unit tracer migrates deeper into the subsurface when ignoring hydromechanical coupling while assuming the hydraulic boundary condition at ground surface is equal to the pressure at the base of an ice-sheet. Hydromechanical coupling acts to increase insitu pore water pressures upon increases in mechanical loading at surface, resulting in decreased vertically downward gradients. In addition, fracture zone interconnectivity and geometry also affect the depth of tracer migration.

Permafrost acts to inhibit recharge during periglacial conditions when the near surface hydraulic conductivity is reduced, while higher TDS concentrations at depth lead to a more stable and density stratified groundwater system with fresh water dominating the near surface portion of the domain.

Groundwater flow models, which do not include a suitable form of hydromechanical coupling, one-dimensional or otherwise, must be used with caution when analyzing a potential DGR site as very large vertical gradients can be generated, resulting in higher predicted pore water velocities, and enhanced migration of surface waters into the subsurface environment.

REFERENCES

[1.] Peltier, W.R., "A design basis glacier scenario," Technical Report 06819-REP-01200-10069-R00, Ontario Power Generation, Nuclear Waste Management Division, Toronto, Canada, 2002.

[2.] Provost, A.M., Voss, C.I., and Neuzil, C.E., "Site-94 – Glaciation and regional groundwater flow in the Fennoscandian Shield," SKI Report 96:11, SKI (Swedish Nuclear Power Inspectorate), Stockholm, Sweden, 1998.

[3.] Boulton, G.S., Kautsky, U., Morén, L., and Wallroth, T., "Impact of long-term climate change on a deep geological repository for spent nuclear fuel," Technical Report TR-99-05, SKB, Stockholm, Sweden, 2001.

[4.] Cedercreutz, J., "Future climate scenarios for Olkiluoto with emphasis on permafrost," Technical Report 2004-06, Posiva Oy, Olkiluoto, Finland, 2004.

[5.] Marshall, S.J., Tarasov, L., Clarke, G.K.C., and Peltier, W.R., "Glaciological reconstruction of the Laurentide ice sheet: Physical processes and modelling challenges," *Canadian Journal of Earth Sciences*, Vol. 37, Iss. 5, 2000, pp. 769–793, doi:10.1139/cjes-37-5-769.

[6.] van der Kamp, G. and Gale, J.E., "Theory of Earth tide and barometric effects in porous formations with compressible grains," *Water Resources Research*, Vol. 19, Iss. 2, 1983, pp. 538–544, doi:10.1029/WR019i002p00538.

[7.] Neuzil, C.E., "Hydromechanical coupling in geologic processes," *Hydrogeology Journal*, Vol. 11, Iss. 1, 2003, pp. 41–83, doi:10.1007/s10040-002-0230-8.

[8.] Jaeger, J.C., Cook, N.G.W., and Zimmerman, R.W., *Fundamentals of Rock Mechanics*, Blackwell Publishing Ltd, fourth edition, 2007.

[9.] Normani, S.D., Park, Y.J., Sykes, J.F., and Sudicky, E.A., "Sub-regional modelling case study 2005-2006 status report," Technical Report NWMO TR-2007-07, Nuclear Waste Management Organization, Toronto, Canada, 2007.

[10.] Frape, S.K. and Fritz, P., "Geochemical trends for groundwaters from the Canadian Shield," in P. Fritz and S.K. Frape (Eds.), *Saline Water and Gases in Crystalline Rocks*, 1987, number 33 in Geological Association of Canada Special Paper, pp. 19–38.

[11.] Peltier, W.R., "Boundary conditions data sets for spent fuel repository performance assessment," Technical Report 06819-REP-01200-10154-R00, Ontario Power Generation, Nuclear Waste Management Division, Toronto, Canada, 2006.

[12.] Srivastava, R.M., "The discrete fracture network model in the local scale flow system for the Third Case Study," Technical Report 06819-REP-01300-10061-R00, Ontario Power Generation, Nuclear Waste Management Division, Toronto, Canada, 2002.

[13.] Srivastava, R.M., "Site2a fracture network models," Compact Disc, 2005.

[14.] Chan, T. and Stanchell, F.W., "DECOVALEX-THMC project: Task E – implications of glaciation and coupled thermohydromechanical processes on Shield flow system evolution and performance assessment, final report," SKI Report 2008:46, SKI (Swedish Nuclear Power Inspectorate), Stockholm, Sweden, 2008.

[15.] McCauley, C.A., White, D.M., Lilly, M.R., and Nyman, D.M., "A comparison of hydraulic conductivities, permeabilities and infiltration rates in frozen and unfrozen soils," *Cold Regions Science and Technology*, Vol. 34, Iss. 2, 2002, pp. 117–125, doi:10.1016/S0165-232X(01)00064-7.